

# Chemorheology of Thermosetting Resins. IV. The Chemorheology and Curing Kinetics of Vinyl Ester Resin

CHANG DAE HAN and KWOK-WAI LEM, *Department of Chemical Engineering, Polytechnic Institute of New York, Brooklyn, New York 11201*

## Synopsis

The rheological properties and curing kinetics of a vinyl ester resin have been determined during isothermal cure. Both steady and oscillatory shearing flow properties were determined using a cone-and-plate rheometer, and the curing kinetics were determined using a differential scanning calorimeter (DSC). Also determined were the rheological properties and curing kinetics of the resin when it had been thickened using magnesium oxide (MgO), in the presence of calcium carbonate (CaCO<sub>3</sub>) as filler and polyvinyl acetate (PVAc) as low-profile additive. The steady shearing flow behavior observed with the vinyl ester resin was found to be very similar to that observed with a general-purpose polyester resin, reported in Paper I of this series [C. D. Han and K. W. Lem, *J. Appl. Polym. Sci.*, **28**, 3155 (1983)]. However, a significant difference in the oscillatory shearing flow behavior was found between the two resins. We have concluded that dynamic measurement is much more sensitive to variations in resin chemistry than steady shearing flow measurement. DSC measurement has permitted us to determine the degree of cure as a function of cure time. By combining the rheological and DSC measurements, we have constructed plots describing how the viscosity increases with the degree of cure, at various isothermal curing temperatures.

## INTRODUCTION

Today, linear unsaturated polyester resin has become one of the most important thermosetting resins used for preparing molding compounds for hot-press matched molding, cold molding, and contact molding. The resin is normally prepared by the reaction of a saturated diol with a mixture of an unsaturated dibasic acid and a "modifying" dibasic acid or its corresponding anhydride. It is commonly referred to as "conventional unsaturated polyester," and typical examples are bisphenol A-fumaric acid polyester and isophthalic polyester. Commercially, the resin is available in the form of solutions containing 60–70 wt % of the prepolymer in a reactive solvent (e.g., styrene).

In conventional polyester resins, the ester groups and carbon-to-carbon double bond linkages are located along the polymer chains, a form referred to as "structopendant,"<sup>1</sup> and they are distributed randomly in the polymer network after the polymer has been crosslinked with styrene. The cured resins are rigid, heat-stable, and have good chemical resistance to most inorganic and organic acids and, also, to a wide range of organic solvents. However, the ester groups and the *unreacted* carbon-to-carbon double bonds in the network provide sites for hydrolytic attack, oxidation, and/or halogenation. This makes the cured resin unsuitable for use in aggressive environments.<sup>2,3</sup>

To overcome these drawbacks much attention has been paid in recent years to the development of resins, which can be fabricated with the same processes

as those for conventional polyester resins, but having superior properties. Vinyl ester resins are the result of such development efforts.<sup>4-6</sup> Vinyl ester resins are addition products of various epoxide resins and ethylenically unsaturated monocarboxylic acids.<sup>5</sup>

They combine the excellent mechanical, chemical, and solvent resistance of epoxy resins with the properties found in the unsaturated polyester resins. In general, cured vinyl ester resin has physical properties superior to cured conventional ester resin, particularly corrosion resistance. This arises from the differences in the number and arrangement of polar groups, such as ester and hydroxyl groups, and carbon-to-carbon double bonds present in the polymer chains.

In vinyl ester resins, the ester groups and carbon-to-carbon double bond linkages are located at the end of the polymer chains, a form referred to as "structoterminal,"<sup>1</sup> and they are distributed uniformly in the network after the polymer has been cured. As a result, cured vinyl ester resin is tougher and has higher resistance to cracking during service than cured conventional polyester resin. Moreover, the distance between crosslinks, i.e., approximately the entire chain length of the prepolymer molecule, is available for absorbing mechanical and/or thermal shocks under stress.

Because of the technological importance of vinyl ester resin, and as part of our continuing efforts to enhance our understanding of the processing-structure-property relationships of thermosetting resins,<sup>7-12</sup> we have very recently carried out an investigation into the chemorheology and curing behavior of vinyl ester resin. In the present study, we have also investigated the effect of viscosity thickener on the chemorheology and curing behavior of vinyl ester resin, in the presence of filler alone, thermoplastic low-profile additive alone or combinations thereof. In this paper, we will report the highlights of our findings.

## EXPERIMENTAL

The vinyl ester resin used in this study was XD-7608.05, an experimental "thickenable" vinyl ester resin produced by Dow Chemical Co. In our previous paper,<sup>8</sup> we reported the effect of viscosity thickener on the rheological properties of the vinyl ester resin, *without* the presence of peroxide. In the present study, we conducted experiments to first investigate the influence of prepolymer chemistry, and then to investigate the influence of the degree of thickening, on the chemorheology and curing behavior of thermosetting vinyl ester resin. The experimental procedure employed is essentially the same as that described in Paper I,<sup>10</sup> except when a viscosity thickener was used. Due to the very high viscosity of the thickened vinyl ester resin (about  $10^4$  P), it was very difficult to mix the thickened resin uniformly with promoter and peroxide. To overcome this difficulty, we prepared the samples by first mixing resin, viscosity thickener, peroxide, filler and/or low-profile additive, but *without* promoter, before thickening taking place at 30°C, and then cured the samples (at various stages of thickening) at elevated temperature. The procedure used in preparing the samples for thickening is described in our earlier papers.<sup>8,9</sup> The composition of the samples used and sample code are given in Table I.

We found that the material that was thickened for over 24 h already cured too fast to permit us to measure meaningful viscosity values, while subjected to

TABLE I  
Sample Code and Material Investigated

Sample code	Material <sup>a</sup>	Cure temp (°C)
(i) Vinyl ester resin		
Fluid 1	Resin/peroxide/promoter <sup>b</sup>	60
(ii) Thickened vinyl ester resin		
Fluid 2	Resin/MgO <sup>c</sup> /peroxide <sup>d</sup>	90
Fluid 3	Resin/MgO/50 wt % CaCO <sub>3</sub> <sup>e</sup> /peroxide	90
Fluid 4	Resin/MgO/20 wt % PVAc <sup>f</sup> /peroxide	90
Fluid 5	Resin/MgO/50 wt % CaCO <sub>3</sub> /20 wt % PVAc/peroxide	90

<sup>a</sup> The amount (wt %) of the additive used is based on resin.

<sup>b</sup> On weight basis, resin/peroxide/promoter = 60/2.0/1.2.

<sup>c</sup> 1 mol MgO (Mod "Me," USS Chemicals) for each mole of prepolymer (see Ref. 8).

<sup>d</sup> On weight basis, resin/peroxide = 60/4.

<sup>e</sup> Camel-wite (A Flinkote Company) treated with a 1.0 wt % silane coupling agent ( $\gamma$ -methacryloxypropyltrimethoxy silane) (Union Carbide, A174).

<sup>f</sup> Solution of 40 wt % poly(vinyl acetate) in styrene (Union Carbide, LP-40A).

shearing motion at an elevated temperature. We suspect that the initiator added might have been decomposed during thickening, making the fluid system into a stage B resin (i.e., a resin that has been partially reacted). We shall elaborate on this point further when we present the results of rheological measurement and differential scanning calorimetry.

The materials which had been thickened for 24 h were used for determining the rheological properties and curing kinetics (both under isothermal conditions), using a cone-and-plate rheometer, and a DSC, respectively. The details of the experimental apparatuses and the procedures employed are described in one of our earlier papers.<sup>10</sup>

With the neat resin/initiator/promoter system (i.e., fluid 1), we conducted both steady and oscillatory shearing flow measurements under isothermal conditions, at various temperatures. With the thickened materials, we conducted only steady shearing flow measurements, under isothermal conditions at 90°C.

## RESULTS

### Steady Shearing Flow Behavior

For fluid 1, cured at 60°C, Figure 1 gives plots of shear viscosity  $\eta$  vs. cure time, and Figure 2 gives plots of first normal stress difference  $\tau_{11} - \tau_{22}$  vs. cure time, with shear rate as parameter.

As shown in Figure 1, the viscosity increases slowly during the early stage of curing and then increases very rapidly, approaching a very large value as the cure progresses. After this very rapid increase, the rate of increase in viscosity starts to slow down at a critical cure time  $t_{\eta_{\infty}}$ . As a matter of fact, when this happened, we noticed *irregular* torque output signals and also noticed an exudation of material from the gap between the cone and plate, indicating that the flow had become unstable. Therefore, from the point of view of rigor, the values of viscosity to the right of the vertical lines in Figure 1 (i.e., above  $t_{\eta_{\infty}}$ ) have little rheological significance.

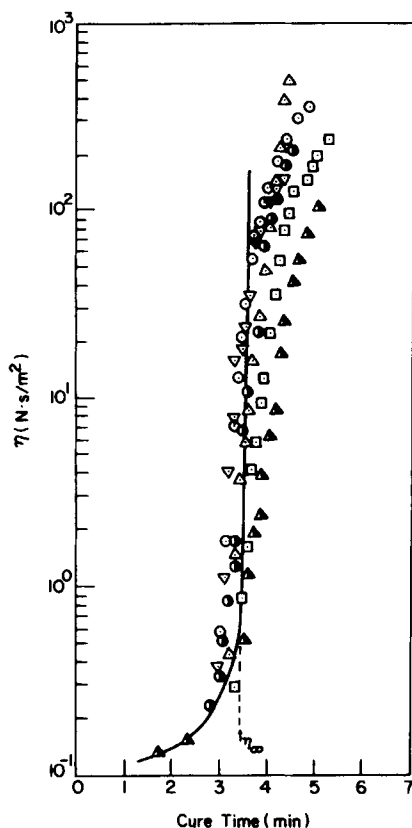


Fig. 1.  $\eta$  vs. cure time at 60°C for neat resin, at various shear rates ( $\text{s}^{-1}$ ): ( $\odot$ ) 0.27; ( $\Delta$ ) 1.07; ( $\square$ ) 2.69; ( $\nabla$ ) 4.27; ( $\bullet$ ) 6.77; ( $\blacktriangle$ ) 17.0.

As discussed in our previous paper,<sup>10</sup> in view of the fact that fluid elasticity develops as the curing reaction progresses (i.e., as the size of the molecules becomes larger due to polymerization), and also in view of the fact that the fluid elasticity increases with shear rate, the deviation of the viscosity–cure time curve from the vertical line at  $t_{\eta\infty}$  may be attributable to the onset of flow instability due to fluid elasticity.

In a manner similar to the situation where we dealt with a general-purpose unsaturated polyester resin,<sup>10</sup> when a sample was placed in the rheometer at rest (i.e., no flow), we observed that the plates were pulled together. This, we believe, is attributable to the shrinkage of the material during cure. The normal force ( $F$ ) measured was used to calculate  $\tau_{11} - \tau_{22} = 2F/\pi R^2$ , in which  $R$  is the radius of the plate. The sign of  $\tau_{11} - \tau_{22}$  is positive when the plates move *apart* from each other. Hence, the negative sign of  $\tau_{11} - \tau_{22}$  in Figure 2 refers to the inward direction of plate movement. Note that, when a sample is subjected to shearing motion, the normal force generated by the motion of the fluid overcomes the shrinkage force and that, at high shear rates,  $\tau_{11} - \tau_{22}$  increases very rapidly with cure time, giving rise to *positive* values, as may be seen in Figure 2.

We realize that, from the point of view of rigor, values of  $\tau_{11} - \tau_{22}$  calculated from the expression,  $\tau_{11} - \tau_{22} = 2F/\pi R^2$ , are of little rheological significance when

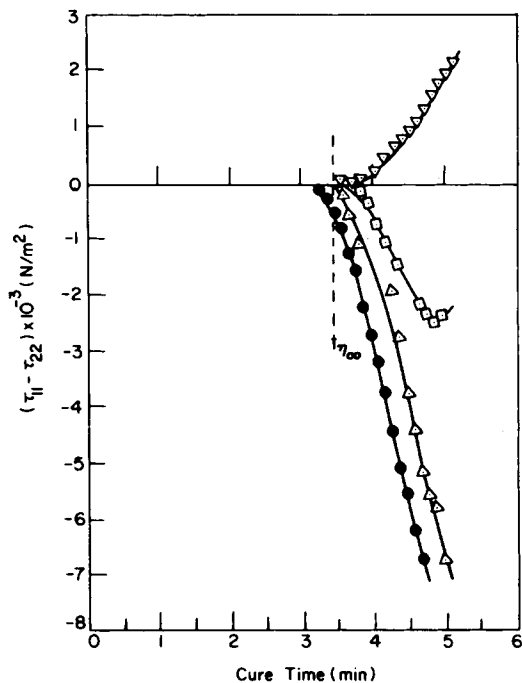


Fig. 2.  $\tau_{11} - \tau_{22}$  vs. cure time at 60°C for neat resin, at various shear rates ( $s^{-1}$ ): (●) 0.0; (Δ) 2.69; (◻) 6.77; (▽) 17.0.

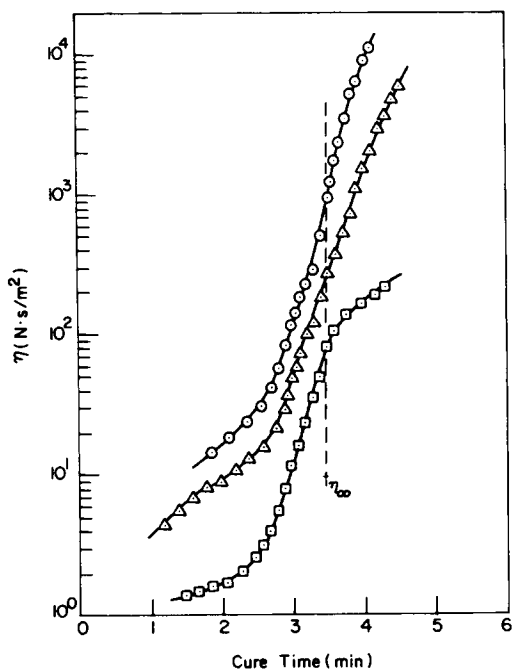


Fig. 3.  $\eta$  vs. cure time at 90°C for thickened resin, at various shear rates ( $s^{-1}$ ): (○) 0.03; (Δ) 1.07; (◻) 2.69.

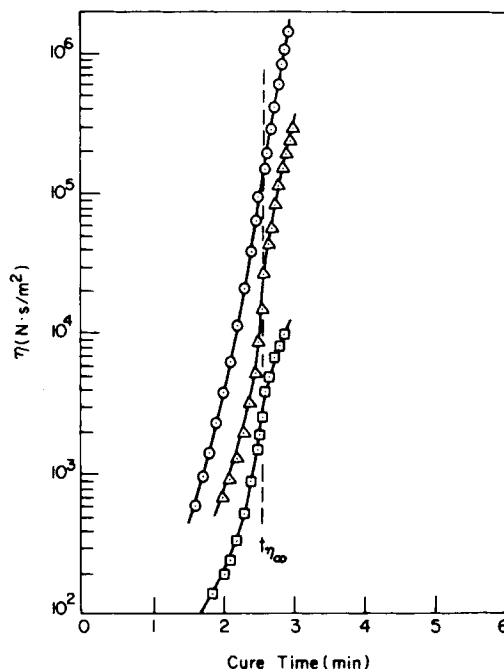


Fig. 4.  $\eta$  vs. cure time at 90°C for thickened resin/ $\text{CaCO}_3$  mixture, at various shear rates ( $\text{s}^{-1}$ ): ( $\odot$ ) 0.03; ( $\Delta$ ) 0.11; ( $\square$ ) 2.69.

the fluid undergoes shrinkage during flow. This is because some of the assumptions made<sup>13</sup> in deriving the expression from the equations of motion are violated. For instance, the available surface area of the fluid undergoing shearing deformation becomes time-dependent when shrinkage occurs. This affects both the boundary conditions and the shape of the fluid at the rim (i.e., the meniscus).

Plots of viscosity versus cure time are given in Figure 3 for the thickened resin (fluid 2), in Figure 4 for the thickened resin/ $\text{CaCO}_3$  mixture (fluid 3), in Figure 5 for the thickened resin/PVAc mixture (fluid 4), and in Figure 6 for the thickened resin/ $\text{CaCO}_3$ /PVAc mixture (fluid 5). It is of great interest to note in Figure 3 that the thickened resin exhibits shear-thinning behavior, whereas the neat resin without additive (see Fig. 1) does not. Note further that the thickened resin has much greater viscosity than the neat resin, in spite of the fact that the thickened resin was subjected to a much higher temperature than the neat resin. The observed difference in viscosity is attributable to the difference in the molecular parameters of the two resins. As mentioned above, we suspect that the initiator (benzoyl peroxide) might have been decomposed slowly during thickening in the presence of  $\text{MgO}$ , and thus the resin might have been polymerized. Therefore, this observed shear-thinning behavior is attributable to the deformation of macromolecules. In a previous paper,<sup>8</sup> we have proposed a mechanism for thickening behavior.

It is seen in Figure 4 that the addition of  $\text{CaCO}_3$  to the resin increases the magnitude of its viscosity and, also, the rate of viscosity increase as the cure progresses. Furthermore, the presence of  $\text{CaCO}_3$  particles in the resin gives rise

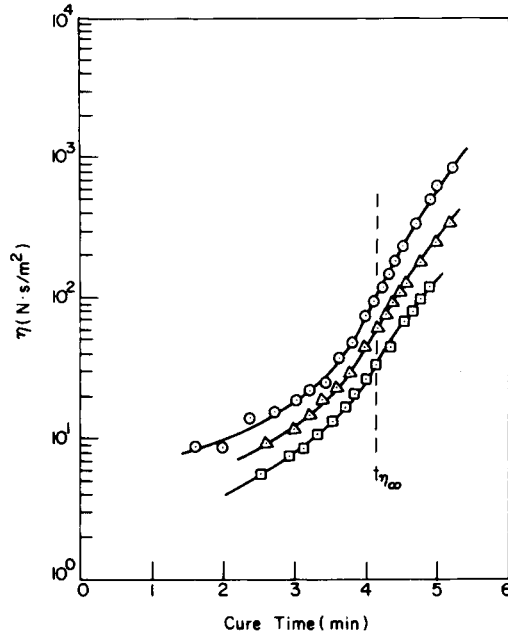


Fig. 5.  $\eta$  vs. cure time at  $90^\circ\text{C}$  for *thickened resin/PVAc* mixture, at various shear rates ( $\text{s}^{-1}$ ): ( $\odot$ ) 0.27; ( $\Delta$ ) 0.68; ( $\square$ ) 2.69.

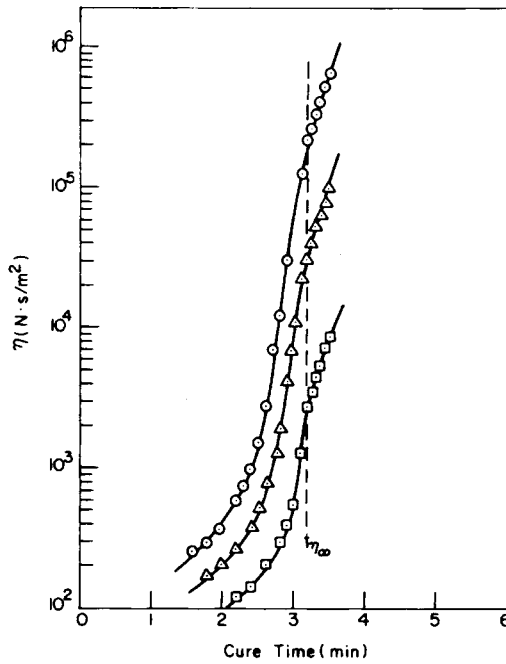


Fig. 6.  $\eta$  vs. cure time at  $90^\circ\text{C}$  for *thickened resin/CaCO<sub>3</sub>/PVAc* mixture at various shear rates ( $\text{s}^{-1}$ ): ( $\odot$ ) 0.03; ( $\Delta$ ) 0.11; ( $\square$ ) 1.07.

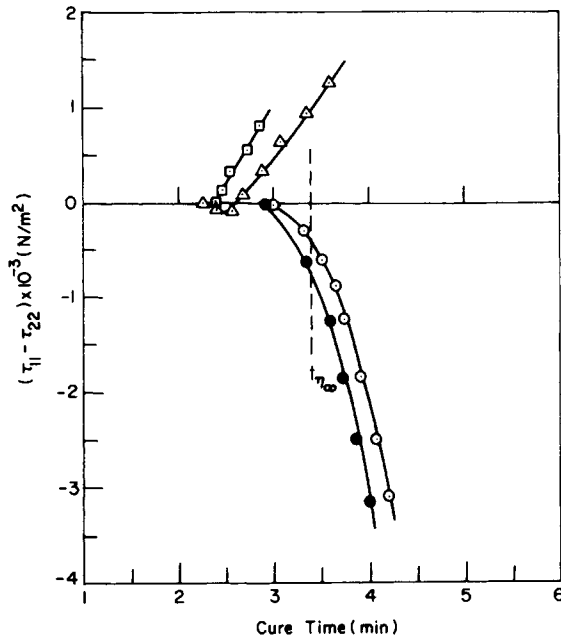


Fig. 7.  $\tau_{11} - \tau_{22}$  vs. cure time at 90°C for thickened resin, at various shear rates ( $\text{s}^{-1}$ ): (●) 0.0; (○) 0.03; (△) 1.07; (□) 2.69.

to shear-shinning behavior. In a previous paper,<sup>11</sup> we have discussed the role of particulates in controlling the viscosity of a resin/particulate mixture during cure.

Figure 5 describes the combined effects of viscosity thickener (MgO) and low-profile additive (PVAc) on the viscosity of the resin/PVAc/MgO mixture during cure. In a previous paper,<sup>12</sup> we have shown that, in the absence of MgO, the resin/PVAc mixture does not exhibit shear-thinning behavior until the cure time reaches a critical value, denoted by  $t_{\eta_{\infty}}$  in Figure 5. It is of interest to note in Figure 5 that the addition of PVAc solution to the resin decreases the rate of viscosity increase as the cure progresses. This is attributable to the fact that, since the PVAc solution contains 60 wt % styrene, the addition of PVAc solution as low-profile additive to the resin dilutes the peroxide initiator and consequently slows down the curing reaction.<sup>12</sup>

Figure 6 describes the variation of viscosity during the cure of the thickened resin in the presence of both  $\text{CaCO}_3$  and PVAc. As expected, the trend of viscosity increase observed in Figure 6 lies somewhere between that of the resin/ $\text{CaCO}_3$  mixture (see Fig. 4) and that of the resin/PVAc mixture (see Fig. 5).

At this juncture, it should be mentioned that the  $t_{\eta_{\infty}}$  shown in Figures 3–6 represents the time at which irregular torque output signals were noticed and must not be construed as the gel time, in the strict sense. As mentioned above in reference to Figure 1, and also in our previous papers,<sup>10–12</sup> the values of viscosity to the right of the vertical line in Figures 3–6 (i.e., above  $t_{\eta_{\infty}}$ ) have little rheological significance, because the flow was no longer, in the strict sense, viscometric during the measurements. Table II gives a summary of  $t_{\eta_{\infty}}$  values for the various fluid systems investigated.



TABLE II  
 $t_{\eta_{\infty}}$ <sup>a</sup> of the Fluids Investigated

Material	Temperature (°C)			
	40	50	60	90
Fluid 1	8.0-8.4	4.4	3.5	—
Fluid 2	—	—	—	3.4
Fluid 3	—	—	—	2.6
Fluid 4	—	—	—	4.2
Fluid 5	—	—	—	3.2

<sup>a</sup>  $t_{\eta_{\infty}}$  is expressed in terms of minutes.

Plots of first normal stress difference  $\tau_{11} - \tau_{22}$  versus cure time are given in Figure 7 for the thickened resin (fluid 2), in Figure 8 for the thickened resin/ $\text{CaCO}_3$  mixture (fluid 3), in Figure 9 for the thickened resin/PVAc mixture (fluid 4), and in Figure 10 for the thickened resin/ $\text{CaCO}_3$ /PVAc mixture (fluid 5). Two things are worth pointing out about the normal stress measurements. First, the thickened resin begins to exhibit positive normal stresses at a shear rate much lower than the value at which the neat resin exhibits them. For instance, as may be seen in Figures 2 and 7, positive values of  $\tau_{11} - \tau_{22}$  are seen at  $\dot{\gamma} = 1.07 \text{ s}^{-1}$  for the thickened resin, whereas negative values of  $\tau_{11} - \tau_{22}$  are seen at  $\dot{\gamma} = 6.77 \text{ s}^{-1}$  for the neat resin. This suggests that the thickened resin, which is a B stage resin, shrinks less than the neat resin, a stage A resin. Second, the thickened resin with  $\text{CaCO}_3$  particles gives rise to a higher rate of  $\tau_{11} - \tau_{22}$  than the thickened resin without  $\text{CaCO}_3$  particles, indicating that the  $\text{CaCO}_3$  particles

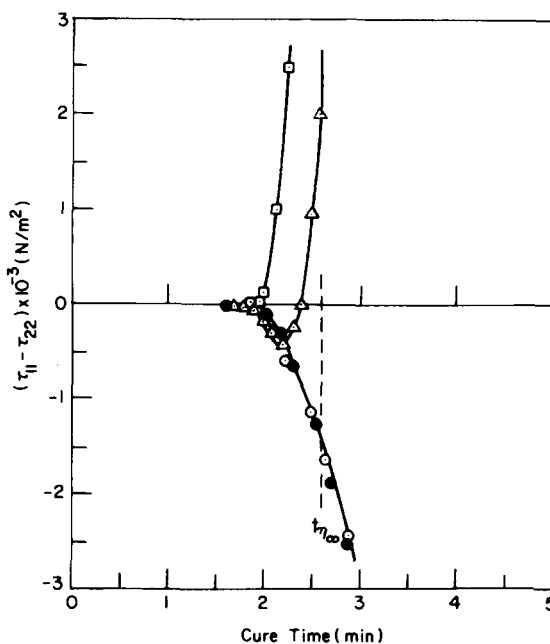


Fig. 8.  $\tau_{11} - \tau_{22}$  vs. cure time at 90°C for thickened resin/ $\text{CaCO}_3$  mixture, at various shear rates ( $\text{s}^{-1}$ ): (●) 0.0; (○) 0.03; (Δ) 1.07; (□) 2.69.

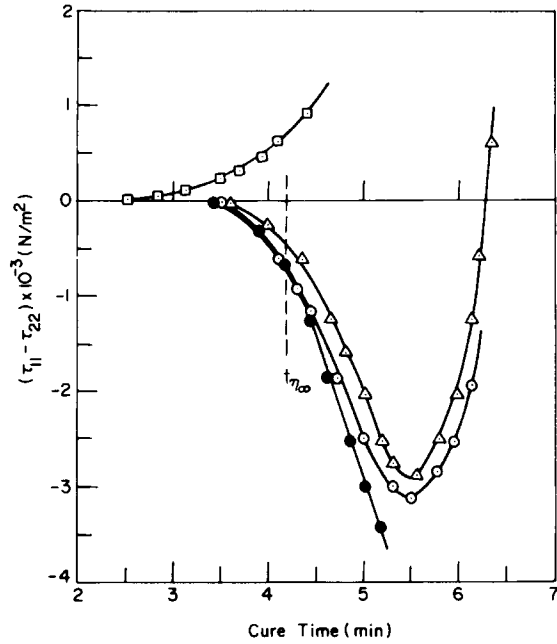


Fig. 9.  $\tau_{11} - \tau_{22}$  vs. cure time at  $90^\circ\text{C}$  for *thickened resin/PVAc* mixture, at various shear rates ( $\text{s}^{-1}$ ): (●) 0.0; (○) 0.27; (△) 0.68; (□) 2.69.

help reduce the shrinkage of the resin during its cure. This observation is in consonance with the observation made earlier with the Ashland general purpose polyester resin.<sup>11</sup>

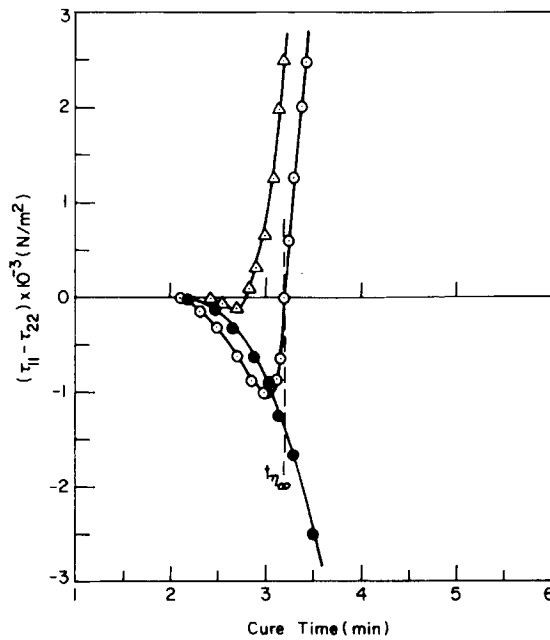


Fig. 10.  $\tau_{11} - \tau_{22}$  vs. cure time at  $90^\circ\text{C}$  for *thickened resin/CaCO<sub>3</sub>/PVAc* mixture, at various shear rates ( $\text{s}^{-1}$ ): (●) 0.0; (○) 0.03; (△) 1.07.

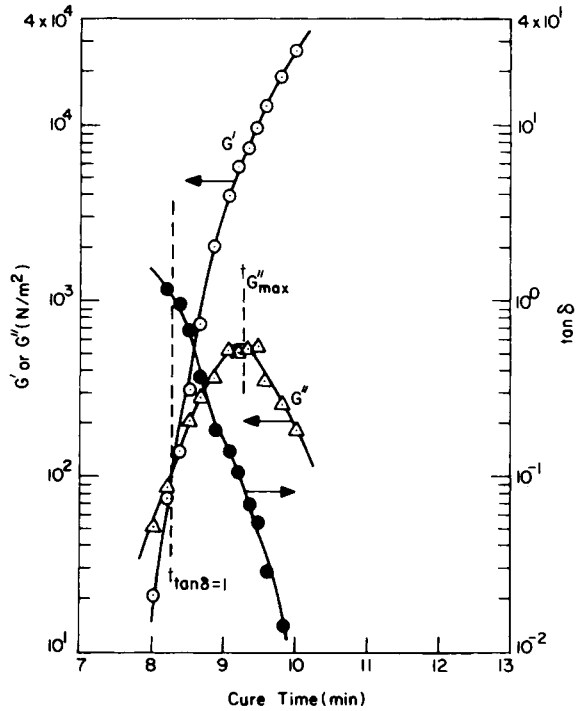


Fig. 11.  $G'$ ,  $G''$ , and  $\tan \delta$  vs. cure time ( $T = 40^\circ\text{C}$ ) for neat resin at  $\omega = 2.99$  rad/s: ( $\odot$ )  $G'$ ; ( $\Delta$ )  $G''$ ; ( $\bullet$ )  $\tan \delta$ .

### Oscillatory Shearing Flow Behavior

Figures 11–14 give the results of oscillatory shearing flow measurements taken at various values of angular frequency, for the neat resin during isothermal curing at  $40^\circ\text{C}$ . It is seen that the storage modulus ( $G'$ ) monotonically increases with cure time at all frequencies tested, and that the slope of the linear portion of the plots,  $d \ln G'/dt$ , increases with decreasing angular frequency, as summarized in Table III.

It is of interest to note in Figures 11–14 that not only the magnitude of the loss modulus ( $G''$ ), but also its shape are strongly dependent upon the frequency imposed on the fluid. Specifically stated, (1) at a given time, the magnitude of  $G''$  increases with frequency; (2)  $G''$  goes through a maximum at low frequency ( $\omega = 2.99$  rad/s) (see Fig. 11); (3)  $G''$  goes through two maxima and a minimum

TABLE III  
Dependence of  $d(\ln G')/dt$  on Angular Frequency

Angular frequency (rad/s)	$d(\ln G')/dt$ ( $\text{min}^{-1}$ )
2.99	5.12
4.74	4.43
7.52	2.96
11.92	2.44
29.94	1.93

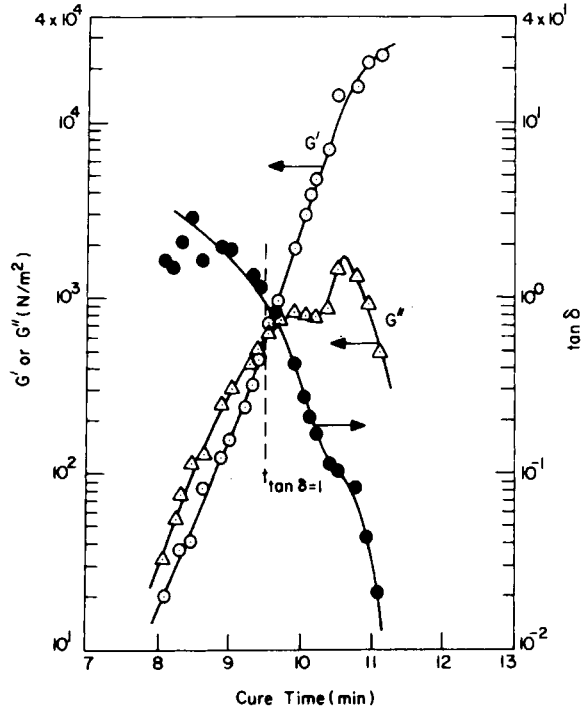


Fig. 12.  $G'$ ,  $G''$ , and  $\tan \delta$  vs. cure time ( $T = 40^\circ\text{C}$ ) for neat resin at  $\omega = 7.52$  rad/s: ( $\odot$ )  $G'$ ; ( $\Delta$ )  $G''$ ; ( $\bullet$ )  $\tan \delta$ .

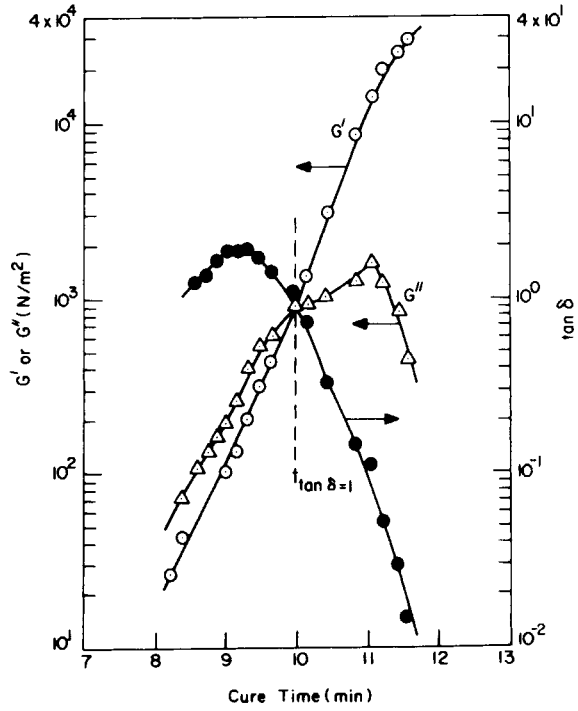


Fig. 13.  $G'$ ,  $G''$ , and  $\tan \delta$  vs. cure time ( $T = 40^\circ\text{C}$ ) for neat resin at  $\omega = 11.92$  rad/s: ( $\odot$ )  $G'$ ; ( $\Delta$ )  $G''$ ; ( $\bullet$ )  $\tan \delta$ .

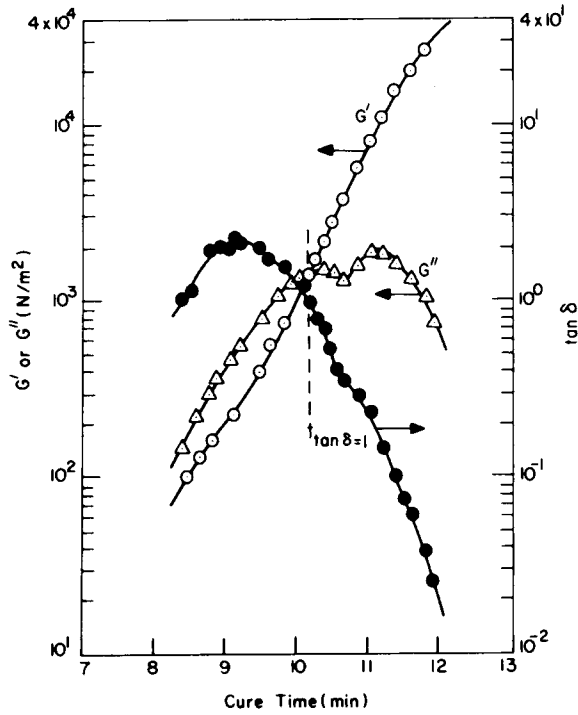


Fig. 14.  $G'$ ,  $G''$ , and  $\tan \delta$  vs. cure time ( $T = 40^\circ\text{C}$ ) for neat resin at  $\omega = 29.94$  rad/s: ( $\odot$ )  $G'$ ; ( $\Delta$ )  $G''$ ; ( $\bullet$ )  $\tan \delta$ .

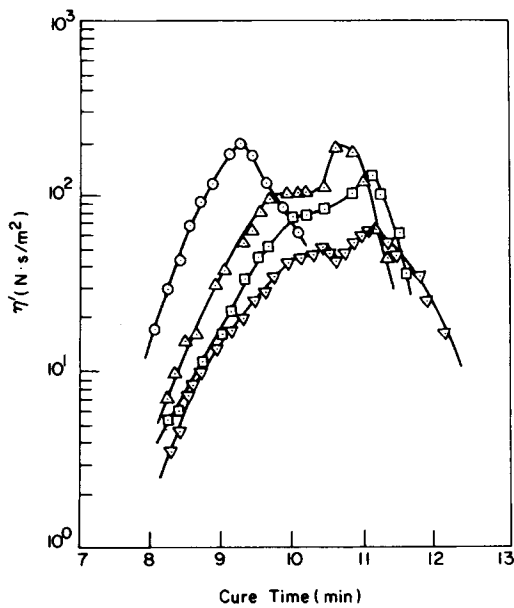


Fig. 15.  $\eta'$  vs. cure time ( $T = 40^\circ\text{C}$ ) at various angular frequencies (rad/s): ( $\odot$ ) 2.99; ( $\Delta$ ) 7.52; ( $\square$ ) 11.92; ( $\nabla$ ) 29.94.

TABLE IV  
Characteristic Time of Vinyl Ester Resin Determined from the Oscillatory Shearing Flow Measurement at 40°C

$\omega$ (rad/s)	$t_{\tan \delta=1}$ (min)	$t_{(G''_{\max})_1}$ (min)	$t_{(G''_{\max})_2}$ (min)	$\Delta t_{(G''_{\max})}$ (min)
2.99	8.30	9.30	9.30	0.00
4.74	8.75	9.00	9.40	0.40
7.52	9.50	9.90	10.50	0.60
11.92	9.95	10.00	11.05	1.05
29.94	10.10	10.35	11.05	0.70

at high frequency ( $\omega = 29.95$  rad/s) (see Fig. 14); (4) at intermediate angular frequencies ( $\omega = 7.52$  rad/s and 11.92 rad/s), the two peaks observed at high frequency appear to overlap each other. Note further in Figures 11–14 that two peaks are observed in the loss tangent ( $\tan \delta$ ) curve at high frequency ( $\omega = 29.95$  rad/s), no peak occurs in  $\tan \delta$  at low frequency ( $\omega = 2.99$  rad/s), and a single peak occurs in  $\tan \delta$  at intermediate frequencies between  $\omega = 29.95$  rad/s and  $\omega = 2.99$  rad/s.

Figure 15 gives plots of dynamic viscosity ( $\eta'$ ) vs. cure time at 40°C, measured at various angular frequencies. Note that  $\eta'$  is the quantity derived from  $G''$  using the relationship  $\eta' = G''/\omega$ . It is seen that the behavior of  $\eta'$  during cure is very similar to that of  $G''$ , with the exception that the magnitude of  $\eta'$  decreases with increasing angular frequency.

Table IV gives a summary of the values of the two characteristic times for the neat resin at various values of angular frequency. These are defined as the time at which the crossover of  $G'$  and  $G''$  occurs ( $t_{\tan \delta=1}$ ) and the time at which the  $G''$  peak occurs ( $t_{G''_{\max}}$ ). Note in Table IV that  $t_{(G''_{\max})_1}$  and  $t_{(G''_{\max})_2}$  refer to the cure times at which the first  $G''$  peak and the second  $G''$  peak, respectively, occur. It is seen in Table IV that the characteristic times initially increase with angular frequency and then level off at  $\omega = 11.92$  rad/s, and that the difference in the cure time between the two  $G''$  peaks,  $\Delta t_{G''_{\max}}$ , goes through a maximum at  $\omega = 11.92$  rad/s.

At this juncture, it should be mentioned that when the vinyl ester resin was cured at temperatures higher than at 40°C, while subjected to oscillatory shearing flow, the output signals were no longer sinusoidal, behavior which is typical of *nonlinear* viscoelastic materials.<sup>13,14</sup> We found that the extent of nonlinearity increases with cure temperature. This is why we have not presented any data on oscillatory shearing flow measurements at cure temperature higher than 40°C.

### DSC Measurement

Figure 16 gives plots of the rate of heat generated ( $dQ/dt$ ) vs. cure time under isothermal conditions, at various temperatures, for neat resin. It is seen that the amount of heat generated (i.e., the area under the  $dQ/dt$ -cure time curve) increases as the cure temperature increases, as would be expected for exothermic chemical reactions.

Figure 17 describes the behavior of the following heat quantities: (1) the heat generated ( $Q_T$ ), obtained by integrating the  $dQ/dt$ -cure time curve given in

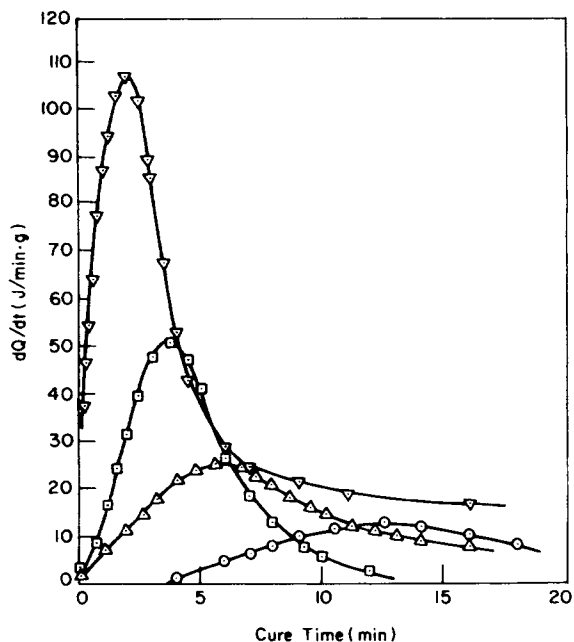


Fig. 16.  $dQ/dt$  vs. cure time for neat resin at various isothermal cure temperatures ( $^{\circ}\text{C}$ ): ( $\odot$ ) 30; ( $\Delta$ ) 40; ( $\square$ ) 45; ( $\nabla$ ) 50.

Figure 16; (2) the heat of curing ( $Q_M$ ) under isothermal conditions, calculated by curve fitting the experimental data to the following quadratic expression:

$$Q_M(T) = C_0 + C_1T + C_2T^2 \tag{1}$$

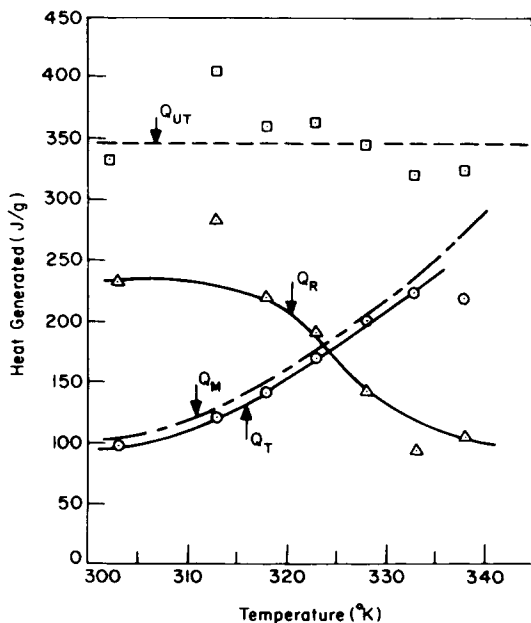


Fig. 17. Heat generated versus isothermal cure temperature for neat resin: ( $\odot$ )  $Q_T$ ; ( $\Delta$ )  $Q_R$ ; ( $\square$ )  $Q_{TOT}$ .

following the suggestion of Kamal and co-workers<sup>15,16</sup>; (3) the residual heat ( $Q_R$ ), which was released when the sample was heated to 200°C, after the completion of an isothermal cure, at a rate of 10°C/min; (4) the total heat of curing ( $Q_{TOT}$ ), which is the sum of  $Q_T$  and  $Q_R$ , i.e.,

$$Q_{TOT} = Q_T + Q_R \quad (2)$$

It is of great interest to note in Figure 17 that the value of  $Q_{TOT}$  turns out to be almost constant.

Following the assumption made by previous investigators<sup>15-19</sup> that the amount of heat generated due to curing is directly proportional to the degree of cure, one can now define:

$$\alpha = Q_i(T)/Q_{UT} \quad (3)$$

where  $Q_i(T)$  refers to the heat generated at a particular time  $t$  at an isothermal curing temperature  $T$  and  $Q_{UT}$  is the ultimate heat of reaction, being the average value of several measurements, taken at various temperatures, of the total heat of reaction  $Q_{TOT}$ .

Figure 18 gives plots of  $\alpha$  versus cure time for the neat resin, and Figure 19 gives plots of the rate of cure (i.e.,  $d\alpha/dt$ ) vs. the degree of cure ( $\alpha$ ). Having constructed plots of  $d\alpha/dt$  vs.  $\alpha$ , we have determined the parameters in the kinetic expression<sup>15,16</sup>

$$\frac{d\alpha}{dt} = (k_1 + k_2\alpha^m)(1 - \alpha)^n \quad (4)$$

A summary of the kinetic parameters in eq. (4) is given in Table V. In calculating these parameters, we assumed a second-order reaction (i.e.,  $m + n = 2$ ) as suggested by Kamal and co-workers<sup>15,16</sup> and used the procedure suggested by Ryan

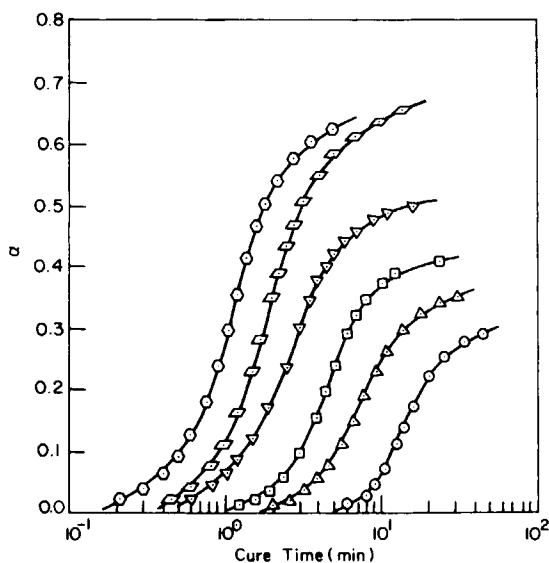


Fig. 18.  $\alpha$  vs. cure time for neat resin at various isothermal cure temperatures (°C): (○) 35; (△) 40; (□) 45; (▽) 50; (◇) 60; (⊙) 65.



TABLE V  
Summary of the Kinetic Parameters Evaluated

Temp (K)	$k_1$ (min <sup>-1</sup> )	$k_2$ (min <sup>-1</sup> )	$m$	$n$
313	0.0054	0.129	0.24	1.76
318	0.0073	0.219	0.33	1.67
323	0.0151	0.998	0.35	1.65
333	0.0624	1.590	0.49	1.51
338	0.0828	1.910	0.51	1.49

and Dutta.<sup>19</sup> It is seen in Table V that, over the range of isothermal curing temperatures investigated, the values of  $m$  and  $n$  are found to be sensitive to temperature, and the values of  $k_1$  and  $k_2$  increase with temperature, following the Arrhenius relationship, with activation energy 103.8 KJ/g-mol for  $k_1$  and 88.1 KJ/g-mol for  $k_2$ .

Having obtained information on the viscosity ( $\eta$ ) and the degree of cure ( $\alpha$ ), both of which vary with cure time (see, for example, Figures 1 and 18), we now can construct plots describing how  $\eta$  varies with  $\alpha$ , as given in Figure 20. It is seen that, as the temperature (more precisely stated, the rate of cure) increases, one can achieve a higher degree of cure before the viscosity approaches a very large value, which was also found in the Ashland general-purpose polyester resin with and without filler.<sup>10-12</sup>

Figure 21 gives plots of  $dQ/dt$  vs. cure time for the *thickened* resin under

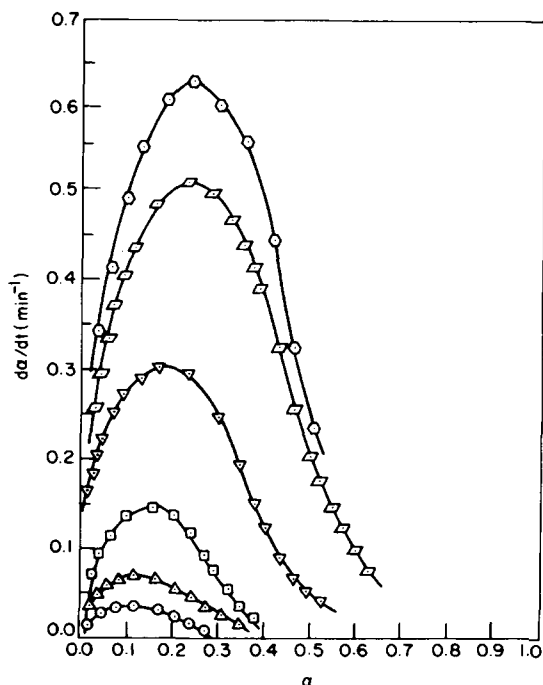


Fig. 19.  $d\alpha/dt$  vs.  $\alpha$  for neat resin at various isothermal cure temperatures (°C): (○) 35; (△) 40; (□) 45; (▽) 50; (◇) 60; (⊙) 65.

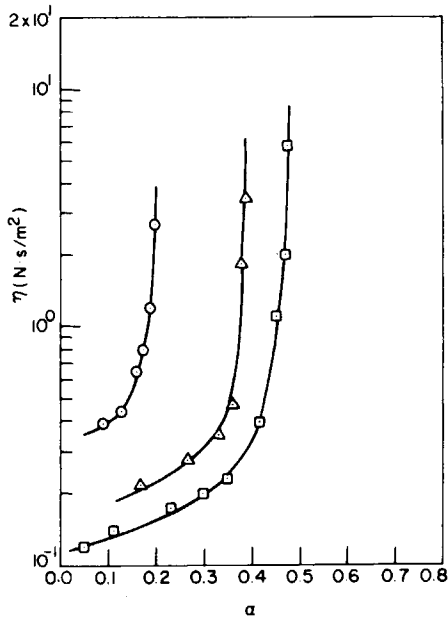


Fig. 20.  $\eta$  vs.  $\alpha$  for neat resin at various isothermal cure temperatures ( $^{\circ}\text{C}$ ). ( $\odot$ ) 40; ( $\Delta$ ) 50; ( $\square$ ) 60.

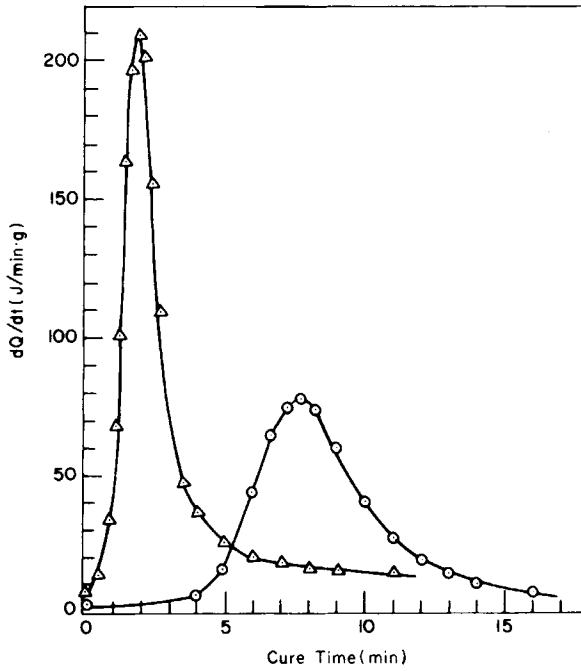


Fig. 21.  $dQ/dt$  vs. cure time for thickened resin at different isothermal cure temperatures ( $^{\circ}\text{C}$ ): ( $\odot$ ) 80; ( $\Delta$ ) 90.

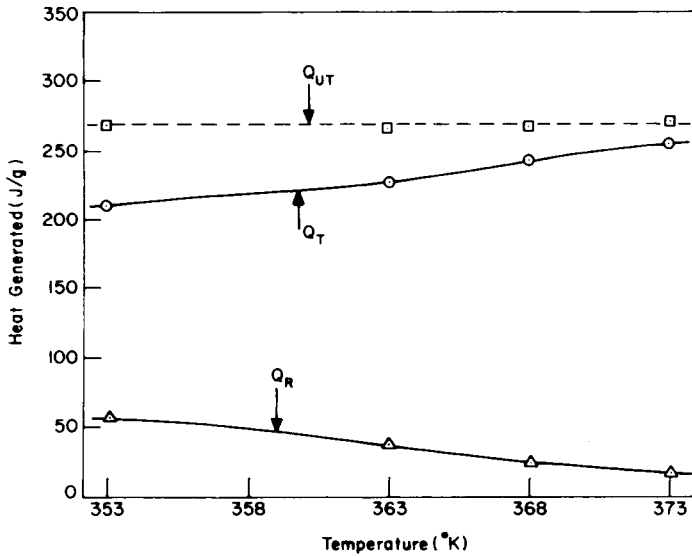


Fig. 22. Heat generated versus isothermal cure temperature for *thickened* resin: (○)  $Q_T$ ; (△)  $Q_R$ ; (□)  $Q_{TOT}$ .

isothermal conditions, at various temperatures, and Figure 22 describes the heat generated by the curing reaction: namely, (1) the heat generated ( $Q_T$ ) by integrating the  $dQ/dt$ -cure time curve; (2) the residual heat ( $Q_R$ ); (3) the total heat

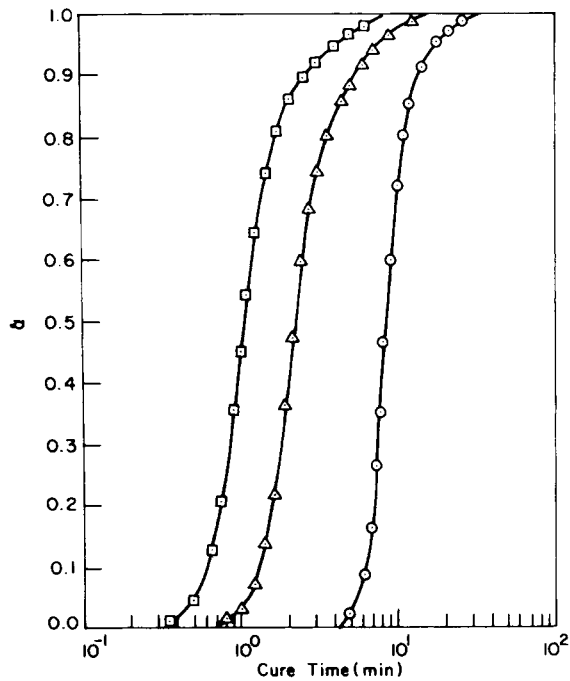


Fig. 23.  $\alpha$  vs. cure time for *thickened* resin at various isothermal cure temperatures (°C): (○) 80; (△) 90; (□) 100.

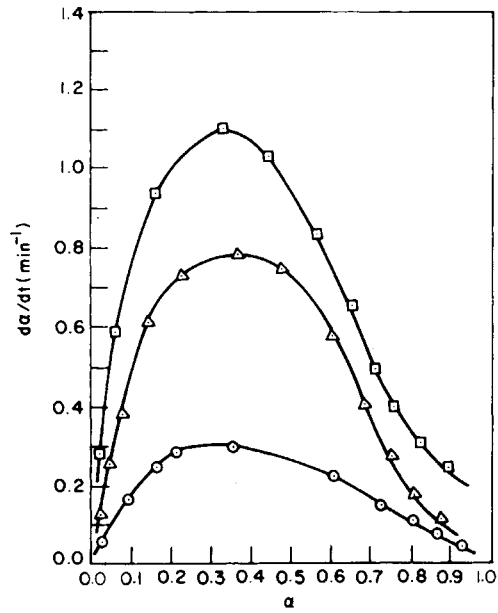


Fig. 24.  $da/dt$  vs.  $\alpha$  for thickened resin at various isothermal cure temperatures ( $^{\circ}\text{C}$ ): ( $\odot$ ) 80; ( $\Delta$ ) 90; ( $\square$ ) 100.

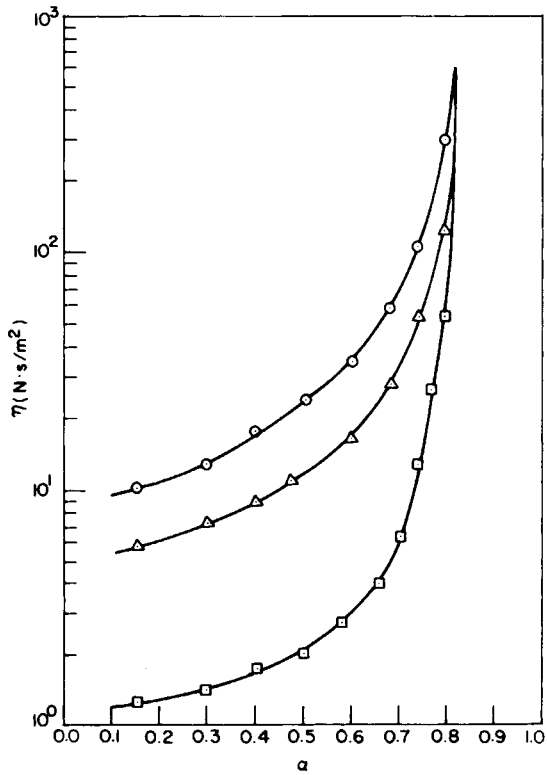


Fig. 25.  $\eta$  vs.  $\alpha$  at  $90^{\circ}\text{C}$  for thickened resin at various shear rates ( $\text{s}^{-1}$ ): ( $\odot$ ) 0.03; ( $\Delta$ ) 1.07; ( $\square$ ) 2.69.

( $Q_{TOT}$ ). Figure 23 gives plots of  $\alpha$  vs. cure time, and Figure 24 plots of  $d\alpha/dt$  vs. cure time, for the *thickened* resin. It is of interest to note that  $Q_{TOT}$  (hence the ultimate heat  $Q_{UT}$ ) of the *thickened* resin ( $Q_{UT} = 268.1$  J/g) is much smaller than that of the *neat* resin ( $Q_{UT} = 345$  J/g) (compare Figures 17 and 22) and that the *thickened* resin attains 100% cure (i.e.,  $\alpha = 1$ ) at about 10 min after cure began at 100°C (see Fig. 23), whereas the *neat* resin attains about 65% cure (i.e.,  $\alpha = 0.65$ ) at approximately the same period after cure began at 65°C (see Fig. 18). Although the curing temperatures were different for the two fluid systems, it appears that the *thickened* resin achieves a greater degree of cure than the *neat* resin. Note that the *neat* resin had a promoter to accelerate the cure at lower temperatures, whereas the *thickened* resin did not contain promoter.

Figure 25 describes how  $\eta$  varies with  $\alpha$  for the *thickened* resin. It is seen that the same value of  $\alpha$  is obtained at lower values of  $\eta$  as the shear rate is increased. This is due to the fact that the viscosity of *thickened* resin is decreased as the shear rate is increased, as may be seen in Figure 3.

## DISCUSSION

### Rheological Behavior during Cure

Although the steady shearing flow behavior observed during the cure of the Dow vinyl ester resin is very similar to that of the Ashland general-purpose unsaturated polyester resin, discussed in Paper I of this series,<sup>10</sup> the oscillatory shearing flow behavior during cure shows significant differences between the two resins. Since we believe that the differences in oscillatory shearing flow arises primarily from the differences in the molecular structure of the two resins, we shall elaborate below on the specific differences observed. They are: (1) the Dow vinyl ester resin shows two peaks in  $G''$  at high angular frequencies and a single peak in  $G''$  at low frequencies, whereas the Ashland polyester resin shows a single peak in  $G''$  at all frequencies tested; (2) the characteristic times (i.e.,  $t_{\tan \delta=1}$  and  $t_{G''_{max}}$ ) obtained for the Dow vinyl ester resin are dependent upon the angular frequency imposed on the fluid, whereas those for the Ashland polyester resin are insensitive to angular frequency; (3) for the Ashland polyester resin,  $t_{\tan \delta=1}$  was found to be almost the same as  $t_{\eta_{\infty}}$  when the resin was cured at low temperature, whereas  $t_{G''_{max}}$  was found to be almost the same as  $t_{\eta_{\infty}}$  when the resin was cured at high temperature (see Ref. 10). On the other hand, for the Dow vinyl ester resin,  $t_{\tan \delta=1}$  coincides fairly well with  $t_{\eta_{\infty}}$  when the resin is cured at low temperature and low frequency, but no relationship is found between the dynamic characteristic times and  $t_{\eta_{\infty}}$  when the resin is cured at high temperature; (4) the output signals for the Dow vinyl ester resin exhibit *nonlinear* characteristics at cure temperatures higher than 40°C, whereas the Ashland polyester resin gives rise to linear output signals over the temperatures tested (up to 60°C). To summarize, we conclude that oscillatory shearing flow measurement is much more sensitive to differences in molecular structure than steady shearing flow measurement.

In an attempt to understand the differences in their oscillatory shearing flow responses, we took measurements of the dynamic mechanical properties of fully cured samples of both the Ashland polyester and Dow vinyl ester resins. The fully cured samples were prepared by first curing a resin at 30°C for 2 h, and

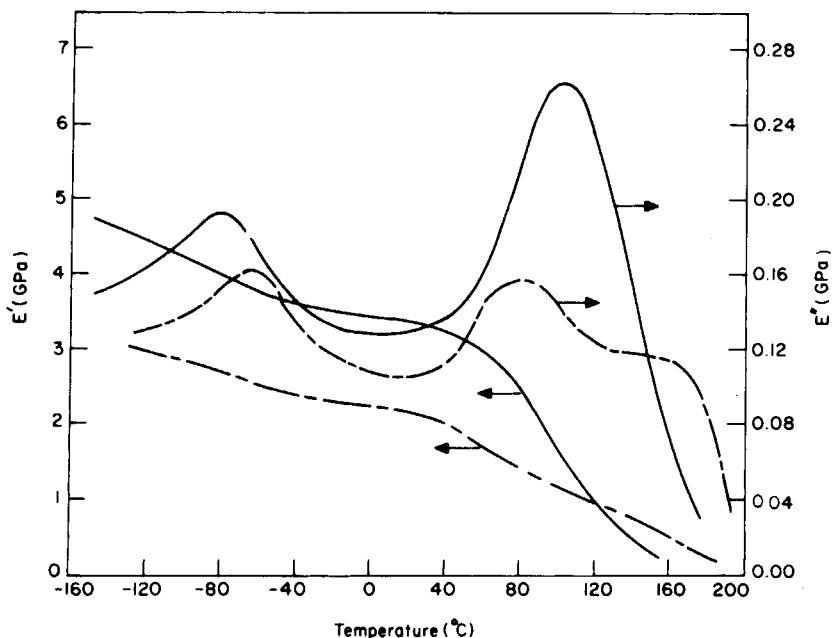


Fig. 26.  $E'$  and  $E''$  vs. temperatures for the Ashland polyester resin (—) and for the Dow vinyl ester resin (- - -).

subsequently post-curing it at 150°C for 12 h under 30 in. Hg vacuum. The dynamic mechanical properties were determined using a DuPont 1090 Thermal Analyzer equipped with a DuPont 981 Dynamic Mechanical Analyzer module.

Figure 26 gives dynamic mechanical spectra (i.e.,  $E'$  and  $E''$ ) of the fully cured samples of both resins. It is seen that the Ashland polyester resin has a higher Young's modulus than the Dow vinyl ester resin, over a wide range of temperatures. The differences in the prepolymer structure of the two resins investigated may be deduced from examining their relaxation transitions (i.e.,  $E''$ ) at both high and low temperatures. Of particular interest is the existence of two major relaxation transitions ( $E''$ ) in the Dow vinyl ester resin at high temperatures. We believe that the second relaxation (occurring at 80°C) is not the same as the  $\beta$ -transition reported in the literature.<sup>20-22</sup> We suspect that the Dow vinyl ester resin investigated in this study might have been a blend of two (or more) resins containing carbon-to-carbon double bonds capable of participating in crosslinking reactions with styrene during cure. We can only speculate at the present time that the observed multiple peaks in  $G''$  of the Dow vinyl ester resin, and its observed nonlinear viscoelastic responses at cure temperatures higher than 40°C when subjected to oscillatory shearing flow, might have arisen from the differences in the reactivity (or crosslinking reaction rate) of each resin, blended with styrene in the preparation of the vinyl ester resin. This speculation will be tested in future investigation.

It is worth noting at this juncture that we believe that the origin of the two peaks in  $G''$  observed with the Dow vinyl ester resin does not lie in gelation and vitrification. Gillham and co-workers<sup>23,24</sup> have investigated the relaxation

transitions of epoxy resins, and assigned the first peak observed to gelation and the second peak to vitrification, using torsional braid analysis (TBA). We understand that the viscoelastic response of the thermosetting resins investigated in their studies was linear over the entire range of cure temperatures. Note, however, that the number and shapes of the  $G''$  peaks observed with the Dow vinyl ester resin we investigated are dependent upon the cure temperature and the angular frequency imposed on the fluid.

### Curing Behavior

Many of the results obtained in the curing of the Dow vinyl ester resin are very similar to those found in the curing of the Ashland general-purpose unsaturated polyester resin, reported in Paper I of this series. Some of the highlights of the curing behavior are: (1) as the cure temperature increases, the maximum value of  $dQ/dt$  in the DSC thermogram increases and the time at which the maximum of  $dQ/dt$  occurs decreases; (2) the degree of cure increases as the cure time increases; (3) the final degree of cure increases with increasing cure temperature.

However, there are important differences in curing behavior. They are: (1) The Ashland polyester resin is more reactive than the Dow vinyl ester resin. (2) The ultimate heat generated by the Dow vinyl ester resin ( $Q_{UT} = 345$  J/g) is greater than that generated by the Ashland polyester resin ( $Q_{UT} = 275$  J/g). (3) The ratio of the residual heat ( $Q_R$ ) to the ultimate heat ( $Q_{UT}$ ) is much higher for the Dow vinyl ester resin than that for the Ashland polyester resin, and thus we can conclude that the Dow vinyl ester resin is less reactive than the Ashland polyester resin, for the same formulation and same initiator system. This conclusion is based on the stipulation that the  $Q_R/Q_{UT}$  ratio may be used as a measure of the amount of *unreacted* functional groups present in the resin, upon completion of an isothermal cure. Note that the  $Q_R/Q_{UT}$  ratio decreases with increasing temperature or rate of reaction. (4) The Ashland polyester resin achieves higher degrees of cure than the Dow vinyl ester resin, upon completion of an isothermal cure.

It should be mentioned that, in determining the kinetic parameters appearing in eq. (4), we have assumed that the curing reaction is of the second order (i.e.,  $m + n = 2$ ). However, as shown in Table V, the values of  $m$  and  $n$  are dependent upon the curing temperature, especially at low temperatures, suggesting that different reaction mechanisms might prevail during low temperature curing.

This work was supported in part by the National Science Foundation under Grant CPE-8211426 and Owens-Corning Fiberglas Corp., for which the authors are very grateful.

### References

1. S. H. Rider and E. E. Hardy, in *Polymerization and Polycondensation Processes*, N. A. J. Platzer, Ed., Advances in Chemistry Series No. 34, American Chemical Society, Washington, D.C., 1962, p. 173.
2. K. J. Saunders, *Organic Polymer Chemistry*, Chapman and Hall, London, 1973.
3. J. A. Brydson, *Plastics Materials*, 3rd ed., Butterworths, London, 1975.
4. D. M. Longenecker, in *Unsaturated Polyester Technology*, P. F. Bruins, Ed., Gordon and Breach, New York, 1976, p. 279.

5. R. E. Young, in *Unsaturated Polyester Technology*, P. E. Bruins, Ed., Gordon and Breach, New York, 1976, p. 315.
6. M. E. Kelly, in *Unsaturated Polyester Technology*, P. E. Bruins Ed., Gordon and Breach, New York, 1976, p. 343.
7. C. D. Han and K. W. Lem, *J. Appl. Polym. Sci.*, **28**, 743 (1983).
8. C. D. Han and K. W. Lem, *J. Appl. Polym. Sci.*, **28**, 763 (1983).
9. K. W. Lem and C. D. Han, *J. Appl. Polym. Sci.*, **28**, 779 (1983).
10. C. D. Han and K. W. Lem, *J. Appl. Polym. Sci.*, **28**, 3155 (1983).
11. K. W. Lem and C. D. Han, *J. Appl. Polym. Sci.*, **28**, 3185 (1983).
12. K. W. Lem and C. D. Han, *J. Appl. Polym. Sci.*, **28**, 3207 (1983).
13. K. Walters, *Rheometry*, Chapman and Hall, London, 1975.
14. S. Onogi and T. Matsumoto, *Polym. Eng. Rev.*, **1**, 45 (1981).
15. M. R. Kamal and S. Sourour, *Polym. Eng. Sci.*, **13**, 59 (1973).
16. M. R. Kamal, S. Sourour, and M. E. Ryan, *Soc. Plast. Eng. Tech. Pap.*, **19**, 187 (1973).
17. G. L. Hagnauer, B. R. LaLiberte, and D. A. Dunn, *Am. Chem. Soc., Div. Org. Coat. Plast., Prepr.*, **46**, 646 (1982).
18. S. Y. Pusatcioglu, A. L. Fricke, and J. C. Hassler, *J. Appl. Polym. Sci.*, **24**, 937 (1979).
19. M. E. Ryan and A. Dutta, *Polymer*, **20**, 203 (1979).
20. K. Tanaka, *Bull. Chem. Soc. (Jpn.)*, **33**, 1702 (1960).
21. W. E. Douglas and G. Pritchard, *J. Polym. Sci., Polym. Phys. Ed.*, **20**, 1223 (1982).
22. W. D. Cook and O. Delatycki, *J. Polym. Sci., Polym. Phys. Ed.*, **12**, 2111 (1974).
23. P. G. Babayevsky and J. K. Gillham, *J. Appl. Polym. Sci.*, **17**, 2067 (1973).
24. J. K. Gillham, J. A. Benci, and A. Noshay, *J. Appl. Polym. Sci.*, **18**, 951 (1974).

Received April 15, 1983

Accepted October 31, 1983